

Characterization of some autoionization resonances in CO₂ using triply differential photoelectron spectroscopy

A. C. Parr and D. L. Ederer

Synchrotron Ultraviolet Radiation Facility, National Bureau of Standards, Washington, D.C. 20234

J. L. Dehmer

Argonne National Laboratory, Argonne, Illinois 60439

D. M. P. Holland

Institute of Physical Science and Technology, University of Maryland, College Park, Maryland 20742

(Received 23 February 1982; accepted 26 March 1982)

We report vibrationally resolved branching ratios and asymmetry parameters for two sets of autoionizing resonances in CO₂ near 680 and 750 Å. These resonances were excited with monochromatized synchrotron radiation from the National Bureau of Standards storage ring and the energy and angle of ejection of the photoelectrons were analyzed. The results show striking non-Franck-Condon behavior.

I. INTRODUCTION

The CO₂ molecule has historically attracted considerable attention in molecular physics for several practical reasons. For example, CO₂ is of central importance in the processes of living systems and the photochemistry of CO₂ is of considerable importance in atmospheric modeling. The disposition of CO₂ in atmospheric modeling in part will determine equilibrium temperatures of the earth. In addition, CO₂ is a constituent of at least one extraterrestrial atmosphere, that of Mars¹⁻³ and photoionization is thought to play a role in the observed emission spectra. In addition to these reasons we have interest in CO₂ as a prototype for photoionization studies in linear triatomic molecules. CO₂⁺ has a rich autoionization structure in the first 8 eV above the ionization onset and we have chosen several isolated resonance regions to map out the effects of the autoionization on the photoionization dynamics in the alternative vibrational ionization channels.

McCulloh⁴ performed a high resolution (0.22 Å) photoionization study of CO₂ and its fragments CO⁺ and O⁺. Earlier studies had suffered from poor spectral resolution or lack of mass discrimination.⁵⁻⁸ McCulloh's photoionization spectra shows a variety of rich structure characteristic of autoionization. This structure is important in the threshold region (~900 Å) and in the region of 650-800 Å with weaker structure elsewhere. Some of the structure has been identified⁹ as high Rydberg states which have as their limits the A, B, and C states of the molecular ion. In particular, we have looked at the sharp autoionizing lines at 753.9, 752.2, and 747.6 Å. The first and third are the *n*=5 members of the Tanaka-Ogawa¹⁰ series with *v*'=0 and *v*'=1, respectively. The major peak at 752.2 Å rises to a cross section value of about 200 Mb and is identified with the *n*=3, *v*'=0 of the Henning sharp series.^{10,11} Recently, Fridh *et al.* have re-examined the assignment on the Henning sharp series and given a lower quantum defect by one unit hence giving this peak a principal quantum number of 3.¹² We will use the more recent designation in this paper. The transitions are further discussed and de-

signed by Fridh *et al.*¹² The Tanaka-Ogawa series has as its limit the A state of CO₂⁺ at 17.32 eV and the Henning sharp series has as its limit the B state of CO₂⁺ at 18.076 eV. In addition, we studied two members at 678.9 and 682.9 Å of the emission and absorption series which have as their limit the C state of CO₂⁺ at 19.39 eV. The first is an absorption minima and is designated *n*=4, *v*'=0 and the second an absorption maxima with *n*=4 and *v*'=0.¹² These lines are summarized in Table I.

We have performed angularly resolved, vibrationally resolved, variable wavelength photoelectron spectroscopy (hence the term triply differential) on these autoionization features. The differential cross section for the photoionization process of an isolated atom or molecule in the dipole approximation can be written

$$\frac{d\sigma_v}{d\Omega} = \frac{\sigma_v}{4\pi} \left[1 + \frac{\beta_v}{4} (3P \cos 2\theta + 1) \right],$$

where σ_v = cross section for the given vibrational channel β_v = corresponding asymmetry parameter for the process, *P* = polarization of light, where *P*=1 would mean the light is entirely horizontally polarized, and θ = angle between the horizontal component of the electric field vector and ejected electron direction in a plane perpendicular to the propagation vector. Assuming the pressure of the sample is constant, the number of electrons ejected per unit light flux *N_v* is proportional to σ_v , hence,

$$\frac{dN_v}{d\Omega} = \frac{N_v}{4\pi} \left[1 + \frac{\beta_v}{4} (3P \cos 2\theta + 1) \right].$$

TABLE I. Autoionizing lines studied here.

λ (Å)	Designation	Limit	Reference
753.9	5 ₀ TO (Tanaka-Ogawa)	A ² Π _u	10
752.2	3 ₀ S (Henning Sharp)	B ² Σ _u ⁺	10, 12
747.6	5 ₁ TO	A ² Π _u	10
682.9	4 ₀	C ² Σ _g ⁺	10, 11, 12
678.9	4 ₀	C ² Σ _g ⁺	10, 11, 12

As a consequence, by measuring the number of electrons as a function of angle, the β parameter and branching ratio can be determined. The branching ratio is just $N_\nu/\sum_\nu N_\nu$ or the fractional number for a given vibrational channel. These numbers can be directly compared to the Franck-Condon factors. The major large scale features of the angular distributions of photoelectrons in CO₂ has been mapped out recently.^{13,14} Swanson *et al.*¹⁵ and Dittman *et al.*¹⁶ have calculated the asymmetry parameter as have the authors of Ref. 14 using the multiple scattering model. The results are in generally good agreement with the results of Refs. 13 and 14. The multiple scattering model is, however, a single electron model with effective potentials and does not deal with the effects of autoionization. In addition, the survey work in Refs. 13 and 14 ignored effects on the fine mesh we report here. Recently, Padial *et al.*¹⁷ have calculated the photoabsorption partial cross section for CO₂ and have calculated the energy levels of the various autoionizing features. Their results are for primarily vibrational averaged measurements and do not directly address the present experiment. Their calculations however do support the spectroscopic designations suggested by Fridh *et al.*¹²

The effects of autoionization on the asymmetry parameters and branching ratios in molecules have been the subject of recent investigations in O₂,¹⁸ CO,¹⁹ N₂,²⁰ and C₂H₂.^{21,22} In all cases, it was found that the branching ratios and the asymmetry parameters varied over the region of a resonance. In addition, in C₂H₂, it was found that additional vibrational modes became excited in resonance regions over what was seen in a 584 Å photoelectron spectrum. This non-Franck-Condon behavior is due to the effect of the intermediate autoionizing state which couples the initial state of the neutral and final state consisting of the ion plus photoelectron.

The 584 Å photoelectron spectrum of CO₂²³⁻²⁷ shows four states with the following adiabatic I.P.'s. The $X^2\Pi_g$ at 13.78 eV, $A^2\Pi_u$ at 17.32 eV, the $B^2\Sigma_u$ at 18.08 eV and the $B^2\Sigma_u^+$ and $C^2\Sigma_g^+$ at 19.39 eV. There is general agreement by the various authors on the energy levels. Work using variable wavelength threshold photoelectron spectroscopy has indicated additional vibrational excitations in the ground state of the molecule ion.²⁵ In addition to determining the Renner parameter, the ν_2 frequency of the ground state of the molecular ion was determined. For the analysis in this study, we will use the values of the vibrational parameters as determined by Frey *et al.*,²⁸ these are $\nu_1 = 1240$ cm⁻¹ and $\nu_2 = 508$ cm⁻¹.

The work reported here consists of stepping through the indicated autoionizing resonances on a small wavelength step (~ 0.5 Å) and recording the angle-resolved photoelectron spectra. The data was subsequently analyzed and values of the asymmetry parameter and the branching ratios derived.

II. EXPERIMENTAL

The major features of the apparatus has been described previously.²⁹ Briefly, the equipment consists of a 2 m normal incidence monochromator at-

tached to the NBS SURF-II storage ring.³⁰ This provides useful monochromatic radiation for ionization experiments from 400 Å upward. Attached to the monochromator is a chamber containing a rotatable 2 in. mean radius hemispherical electron energy analyzer. The analyzer is operated in a mode such that when combined with a monochromator band pass of 0.5 Å the net electron energy resolution is about 120 meV. It should be noted, however, that for purposes of studying fine structure in the absorption spectra, the important factor is determined by the resolution of the monochromator.

The light intensity and polarization is continuously monitored during the course of an experiment with a set of tungsten photodiodes and a triple reflection gold surfaced polarization analyzer. A typical experiment consisted of selecting a particular wavelength and obtaining photoelectron spectra at three different angles with respect to the major axis of the partially polarized light. The three angles were used for redundancy and as a check for systematic errors. The data is stored on floppy disks by a LSI-11 Camac based data acquisition system for later analysis.

The analysis consists of a fit to a set of Gaussian base functions using the vibrational parameters suggested by Frey *et al.*²⁸ The fit involves a nonlinear least-squares analysis to the assumed form where the widths and amplitudes are free parameters. In general, this program converges to a common value for width so that these parameters can usefully be fixed to expedite analysis. The spectrometer system is calibrated for energy and angle as discussed by Holland *et al.*³¹ The program for fitting utilizes the various corrections and calculates branching ratios and asymmetry parameters from the parameters generated by the fit.

The sample was a commercially obtained sample of 99.8% stated purity. The gas was used without further purification. The sample pressure in the chamber was on the order of 5.0×10^{-5} Torr. The pressure in the interaction region was higher due to the directed nature of the inlet jet. A capillary light tube 12 in. long isolates the experimental chamber from the monochromator and storage ring which are thereby maintained at least three orders of magnitude lower in pressure.

III. RESULTS AND INTERPRETATION

The principle vibrational progressions in the ground state of CO₂⁺ are the $(n, 0, 0)$ transitions with Franck-Condon factors of 0.82 for the $(0, 0, 0)$, 0.15 for the $(1, 0, 0)$, and 0.02 for the $(2, 0, 0)$.³² A theoretical discussion of the Franck-Condon factors in CO₂ is given by Sharpt and Rosenstock.³³ Turner³² gives a value of 0.017 for the Franck-Condon factor for the $(0, 0, 2)$ mode. It is apparent from inspection of Fig. 1 that the simple $(n, 0, 0)$ progression does not adequately describe the photoelectron spectra at this wavelength. This spectrum was taken in the region of the $n=3$, $v=0$ member of the Henning Sharp series which has as its limit, the B state of CO₂⁺. The solid vertical lines represent the positions of the $(n, 0, 0)$ levels with the line through the

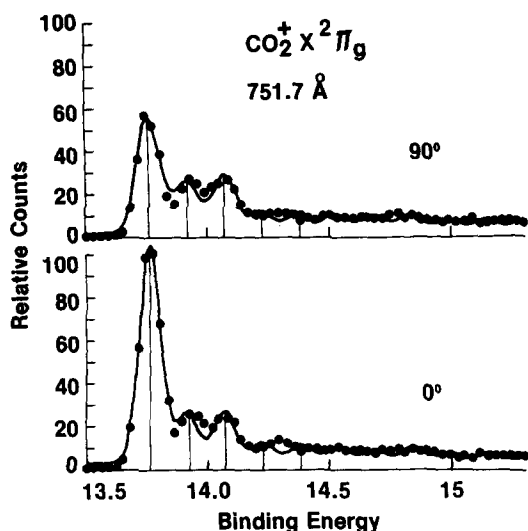


FIG. 1. Photoelectron spectra of CO₂ taken at a wavelength of 751.7 Å. The vertical scale is electron counts per unit energy per unit light flux in arbitrary units. The heights are adjusted to 100 for the largest value. The solid vertical lines are the positions of the first five vibrational levels of the v_1 series used in the fit. The solid line represents the computed fit to the data.

points being the best fit with this set of parameters. Clearly, at about 14 and 14.3 eV the structure is not adequately accounted for. The inability of the analysis to correctly account for the observed structure suggests that the single non-Franck-Condon progression model is inadequate. Several things were tried to improve the fit, including allowing for excitation of a quantum of the v_2 and v_3 vibration. The approach that seemed to yield the best fit was allowing for single excitation of the v_2 mode for excitation of the v_1 mode with $n=1, 2$, and 3 quanta of excitation. To account for the high binding en-

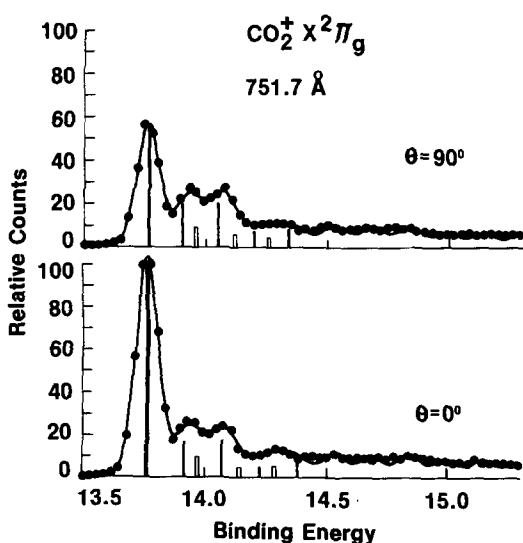


FIG. 2. The same data and axes as in Fig. 1. The solid bars represent position and relative amplitude of the main v_1 vibrational progression in the fit. The open bar represents the three vibrational levels of the form $(n, 1, 0)$ of the v_2 progression needed to fit the data.

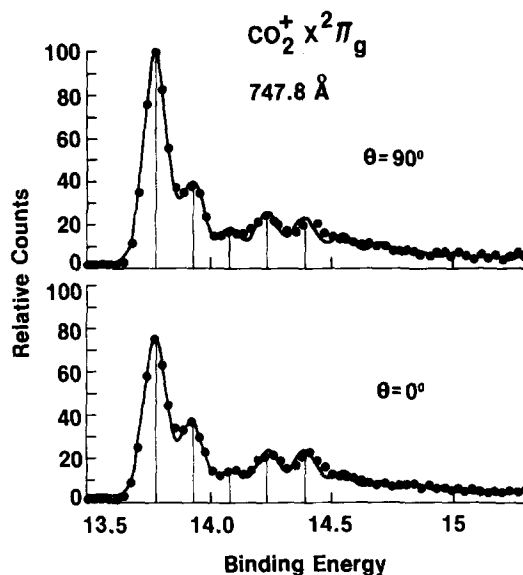


FIG. 3. Photoelectron spectra of CO₂ taken at 747.8 Å, 86 meV from that of Figs. 1 and 2. This is the region of a smaller peak near the large resonance at 752.2 Å. The scales are the same as in Fig. 1. The data was fit rather well with a simple model of a v_1 progression with very non-Franck-Condon behavior.

ergy tail visible in Fig. 1, values of the quantum number for the principle progression of up to ten were used. This tailing was real and cannot be attributed to scattering or other experimental artifacts. This structure was unresolved and hence could be due to other vibrational excitation as well. The principal progression was used to obtain an estimate of the total intensity. The amplitudes of the higher members of the progression are not plotted in the figure since their identification is uncertain. Photoelectron spectra taken away from these resonance positions did not show this behavior.

The use of a single quanta of excitation of the v_2 mode violates the normal selection rules as would a model giving single excitation of the v_3 mode. The inescapable conclusion of the present fitting test was, however, that a selection rule breaking transition was involved and the best fit is given when v_2 excitation is involved. Frey *et al.*²⁸ found the v_2 excitation in single quanta in their threshold photoelectron spectra of CO₂ as well.

The result of including these excitation is shown in Fig. 2. The computed fit fits most of the data extremely well. The positions and relative strengths of the additional levels are shown in the open bars. It should be noted that it was unnecessary to include the excitation $(0, 1, 0)$. Attempts to do this resulted in poorer fits. The heights of the solid and open bars represent the intensities given to the excitations at these points. This type of fit was necessary in the region of the major absorption peak (752.2 Å). Away from this narrow region, there was no evidence for the additional excitation among the wavelengths studied in this work.

Figure 3 gives the photoelectron spectrum taken near the $n=5, v=1$ state which has as its limit the A state of

CO₂. Even though the intensity pattern is very non-Franck-Condon, the spectrum can be accounted for by the varying intensities of the principle vibrational progression. The same was observed for the window region around 680 Å. In all of the regions studied, the lack of complete resolution made the determination of the substructure somewhat ambiguous. There is evidence for selection rule breaking transitions in the photoionization of CO₂²⁸ but the intensities and lack of the (0,1,0) mode in one case are not readily explained. The fitting routines used here and the appearance of the spectra do indicate a substantial substructure but the unambiguous determination of the exact nature will await

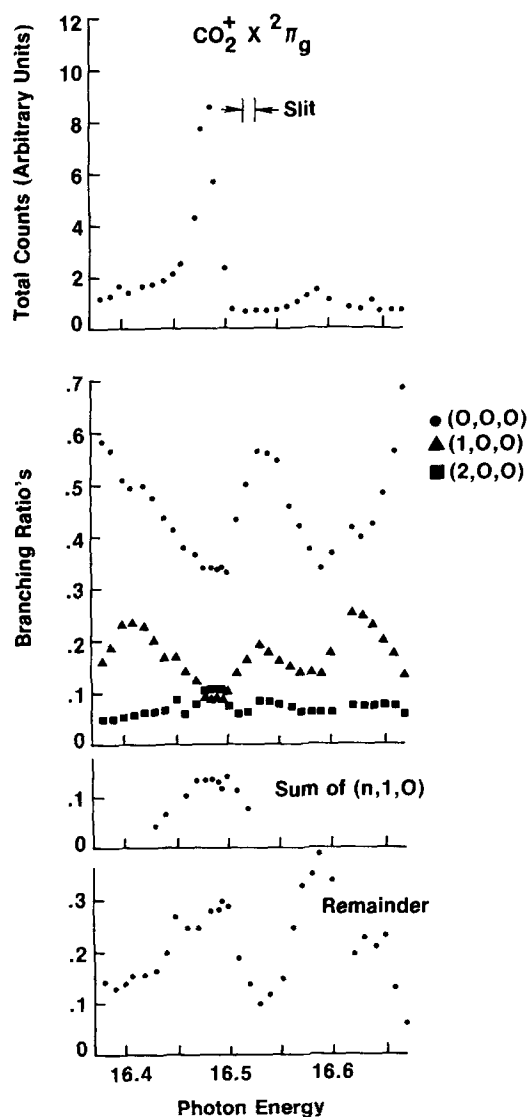


FIG. 4. The CO₂⁺ X ²Π_g vibrational branching ratios and total electron count for the resonance in the 750 Å region. The branching ratios are the fraction of a given peak area to the total electron intensity in the 1.6 eV electron energy range spanned in Figs. 1–3. It should be noted from Figs. 1–3 that the photoelectron spectra do not go to zero at higher binding energies, indicating there are still other vibrational excitations ignored here. The designation (0,0,0) means $v_1=0$, $v_2=0$, $v_3=0$ for the state of the ion given. The sum (n,1,0) indicates the sum of the substructure where $n=1-3$. The remainder is the residual intensity not accounted for in the other designated curves.

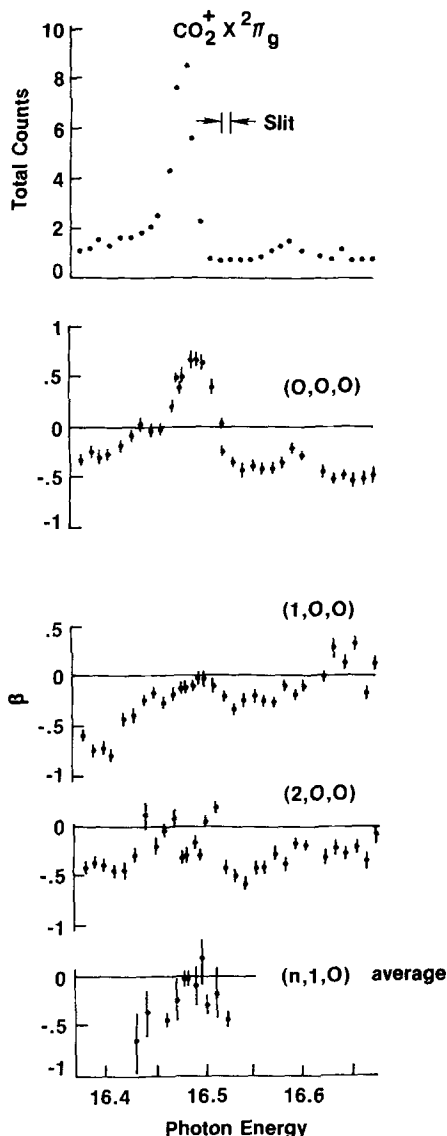


FIG. 5. The CO₂⁺ X ²Π_g asymmetry parameters β for the 750 Å region resonances. The top figure is total electron count for use as a reference. The graphs are labeled as described in Fig. 4.

higher resolution experiments. The main features of the discussion, however, are not substantially altered by this.

IV. 750 Å REGION

The wavelength dependent results for this region analyzed as discussed above are shown in Figs. 4 and 5. Figure 4 gives the total counts (integrated over the CO₂⁺ X ²Π band) and branching ratios as a function of photon energy. The total counts follow the same general shape as the photoionization curve of McCulloh. The slit width of the monochromator is shown. The 5₀TO member of the Tanaka-Ogawa series at 16.445 eV is not clearly resolved. The 5₁TO series member is at 16.58 eV and is resolved. The main peak is the 3₀S member of the Hennings sharp series.

The branching ratios for the first three levels of the v_1 progression are shown, as is the sum of the branching

ratios of v_2 series. The final graph shows the intensity in the remaining unresolved structure at higher binding energy which is presumably due mainly to higher members of the v_1 progression with possibly v_2 excitation and other modes and combinations as well. Near the resonances, the (0,0,0) and the (1,0,0) intensities drop considerably from the background levels of approximately the Franck-Condon values of 0.82 and 0.15, respectively. The intensity in the substructure attributed to the v_2 series rises in the region of the 3_0S level and makes insignificant contributions elsewhere. The remainder rises in regions of all the resonances including the small bump at 16.45 eV which is due to the 5_0TO level which is not clearly resolved in the total cross section as given at the top of the figure.

Whatever the exact nature of the substructure which we have attributed to the v_2 vibrations, it only effects the $X^2\Pi_g$ ground state when it is populated by the 4_0S level of the Henning series. This would suggest that this member of the Henning series contains distortions from linearity which allows for the population of the antisymmetric modes of the $X^2\Pi_g$ ground state. The other thing to note is that very high vibrational members of the v_1 progression are being excited via the autoionization even though the vibrational quantum numbers of the autoionizing levels are 0 and 1. Note that this example of electronic autoionization does not follow this propensity rule in vibrational autoionization which suggests the smallest possible Δv .³⁴

Figure 5 gives the v -dependent photoelectron asymmetry parameter β for this region of the spectra. The (0,0,0) level has a background value of about -0.4 on the low energy side and of about -0.5 on the high energy side. Grimm *et al.*¹⁴ give a value of -0.33 for the (0,0,0) level at 750 Å (16.351 eV). Their resolution was 2 Å which integrated a portion of the data shown here but nevertheless gives a comparison. This is the only directly comparable β value. The β value increases above background for all three autoionizing levels but particularly so in the region of the 3_0S level. There is structure in the value of β for the vibrational modes (1,0,0) and (2,0,0) in the regions of the autoionization as well. The bottom graph in the figure is given for completeness only. The values for β depend sensitively upon the calculated peak heights by the fitting routine and since the structure is not clearly resolved, the error in these β 's is large. The changes in β are significant if it is kept in mind that the total range possible for β is +2 to -1.

V. 680 Å REGION

The branching ratios for the window and absorption series in the 680 Å (18.23 eV) region is shown in Fig. 6. The top graph is the photoionization efficiency of McCulloh⁴ normalized to the absorption cross section measured by Lee and Judge.³⁵ Our measured normalized total photoelectron count does not follow the intensity profile that the total photoionization cross section does. This is most likely due to the fact that competing decay mechanisms can lead to depopulation of the excited autoionizing levels. The energy of these resonances is above the energy of the X , A , and B states

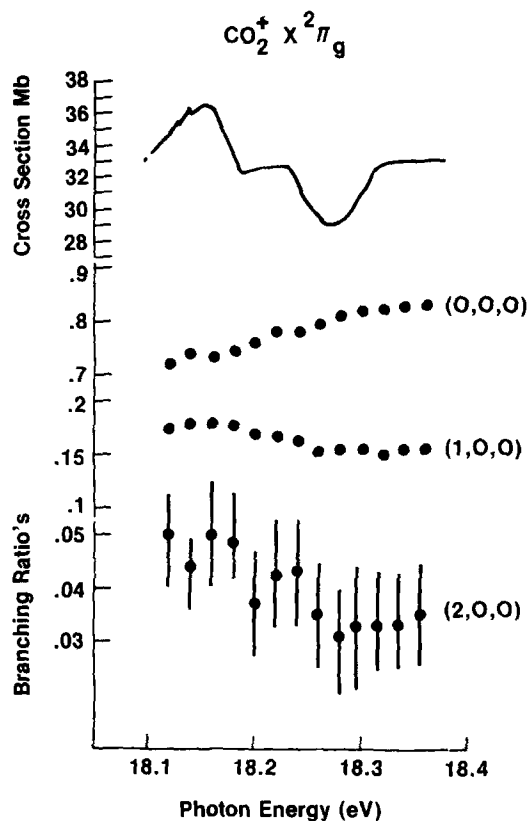


FIG. 6. The branching ratios for the $CO_2^+ X^2\Pi_g$ in the vicinity of the resonances near 680 Å. The cross section as derived from the literature is shown at the top. See the text for details. The curves are labeled as in Fig. 4.

of molecular CO_2^+ . As a consequence, the autoionizing levels can selectively decay to the various states and this may well be a function of energy. Baer and Guyon have found this to be the case in a similar resonance in CO_2 they studied at a 18.67 eV.³⁶ They found that there is a competition between direct decay to the ground state and fluorescent channels via the A and B state. These rates were found to vary as a function of the photon energy. The elucidation of these processes will await a future study.

The branching ratios shown in Fig. 6 do not show any rapid fluctuations characteristic of the autoionization lines. The intensities in this region are not far removed from the Franck-Condon values for the vibrational transition amplitudes. The asymmetry parameters shown in Fig. 7 do show variation, particularly the weaker vibrational members.

The photoelectron spectra were fit quite adequately by a simple model of the v_1 progression. The amplitude of peaks with quanta greater than three was almost negligible, hence, all the amplitude was in the first three or four peaks with no substructure discernable, quantitatively different from the peaks in the 750 Å region.

CONCLUSION

We have mapped the variation of vibrational branching ratios and the v -dependent asymmetry parameters

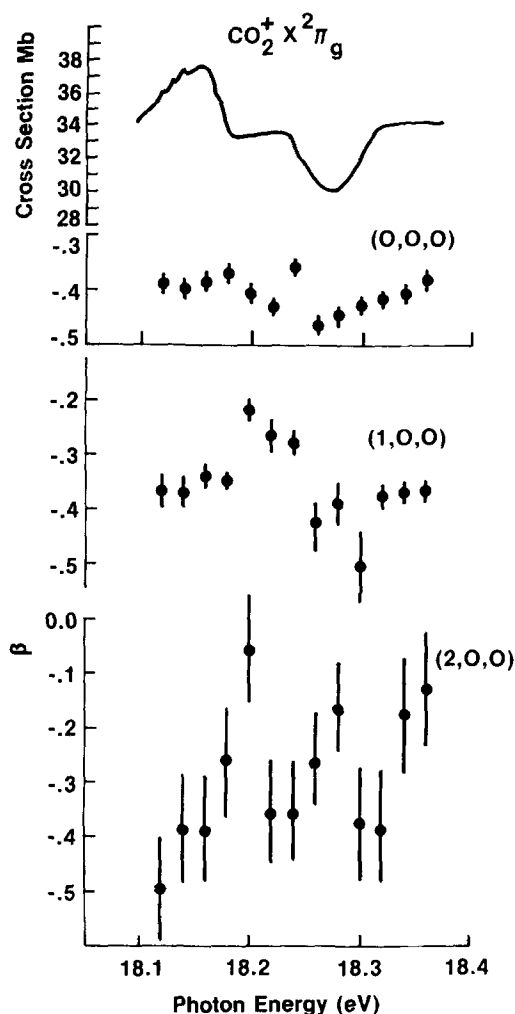


FIG. 7. The v -dependent asymmetry parameters for the $\text{CO}_2^+ X^2\Pi_g$ state for incident radiation in the 680 Å region. The curves are labeled as in Fig. 4.

within two types of autoionization resonances in CO_2^+ . The first at 750 Å could only interact with continua from the ground state manifold, whereas the second at 680 Å could interact with the continua of several electronic states. It is apparent from this first look that situations like the latter will demand a complete look at all the decay channels to parametrize the reaction. At this time, there is no complete theory of autoionization and its effect on branching ratios and asymmetry parameters. For example, the multiple scattering model³⁷ has had considerable success in predicting the qualitative effects of shape resonance upon the vibrationally resolved branching ratios and asymmetry parameters but does not address multielectron processes such as autoionization. Dill and Jungen,³⁸ and Roault and Jungen³⁹ have worked out a detailed theory for the photoionization of molecular hydrogen. The theory uses spectroscopically determined parameters and multichannel quantum defect theory. The resulting differential cross section contains information on the appropriate transition amplitudes and phases for alternately accessible vibrational channels in that molecule. The theory was successful in fitting the available photoionization data⁴⁰ on relative cross sections but remains experimentally untested with re-

gard to branching ratios and asymmetry parameters. Other developments^{41,42} in the area of computing vibrationally resolved molecular photoionization have occurred recently, however, none have proceeded enough to account for the autoionization effects such as those observed here, except in the case of H_2 . We hope that the present data helps stimulate progress in that direction.

The complexity of molecular photoionization demands that a theory of the autoionization be able to account for the additional interactions and decay channels that a molecule has in addition to electronic de-excitation. In particular, the vibrational coupling between the autoionizing transition state and the initial and final state must be accounted for. The mediation of the photoionization process by the autoionizing state allows the electronic motion to exchange energy and angular momenta with the nuclear motion. This results in vibrational intensity distributions and even in additional modes of excitation in molecules which are not predictable by application of the Franck-Condon principle. As shown here, the 752.2 Å absorption line in CO_2 generates vibrational populations of $\text{CO}_2^+ X^2\Pi_g$ differ drastically from those in the 584 Å spectra. As a consequence, the resulting infrared de-excitation of the ground state will have additional components and intensities. In the case of the 750 Å region autoionization, there was qualitative differences between the additional excitation due to the three autoionization lines. This could be interpreted as being due to different geometries of the Rydberg levels and a different coupling to the $\text{CO}_2^+ X^2\Pi_g$ ground state. In the case of the 680 Å resonances, the problem even becomes more complex because of the competition between the various final state continua and fluorescent channels. The types of measurements to be made which will enable a complete characterization of the dynamics of molecular photoionization against which theoretical developments can be tested.

ACKNOWLEDGMENTS

We wish to thank Dr. R. P. Madden for his support and encouragement throughout this work and Dr. Henry Rosenstock and Dr. Roger Stockbauer for suggestions and aid in various aspects of the work. This work was supported in part by the Office of Naval Research, the U.S. Department of Energy and NATO Grant No. 1939.

¹C. A. Barth, W. A. Fastie, C. W. Hord, J. B. Pearce, G. E. Thomas, G. P. Anderson, and O. F. Raper, *Science* **165**, 1004 (1969).

²C. A. Barth, C. W. Hord, J. B. Pearce, K. K. Kelly, G. P. Anderson, and A. I. Stewart, *J. Geophys. Res.* **76**, 2213 (1971).

³A. I. Stewart, *J. Geophys. Res.* **77**, 54 (1972).

⁴K. E. McCulloh, *J. Chem. Phys.* **59**, 4250 (1973).

⁵N. Wainfan, W. C. Walker, and G. L. Weissler, *Phys. Rev.* **99**, 542 (1955).

⁶R. S. Nakata, K. Wantanabe, and F. N. Matsunaga, *Sci. Light (Tokyo)* **14**, 54 (1965).

⁷V. H. Dibeler and J. A. Walker, *J. Opt. Soc. Am.* **57**, 1007 (1967).

- ⁸For a review of the photoionization and absorption spectroscopy, see Ref. 4.
- ⁹E. Lindholm, Ark. Fys. **40**, 125 (1969).
- ¹⁰Y. Tanaka and M. Ogawa, Can. J. Phys. **40**, 829 (1962).
- ¹¹Y. Tanaka, A. S. Jursa, and F. J. LeBlanc, J. Chem. Phys. **32**, 1199 (1960).
- ¹²C. Fridh, L. Asbrink, and E. Lindholm, Chem. Phys. **27**, 169 (1978).
- ¹³T. A. Carlson, M. O. Krause, F. A. Grimm, J. D. Allen, D. Mehaffy, P. R. Keller, and J. Taylor, Phys. Rev. A **23**, 3316 (1981).
- ¹⁴F. A. Grimm, J. D. Allen, T. A. Carlson, M. O. Krause, D. Mehaffy, P. R. Keller, and J. Taylor, J. Chem. Phys. **75**, 92 (1981).
- ¹⁵J. R. Swanson, D. Dill, and J. L. Dehmer, J. Phys. B **14**, L206 (1981).
- ¹⁶D. Dittman, D. Dill, and J. L. Dehmer (to be published).
- ¹⁷N. Padial, G. Csank, B. V. McKoy, and P. W. Langhoff, Phys. Rev. A **23**, 218 (1981).
- ¹⁸K. Codling, A. C. Parr, D. L. Ederer, R. Stockbauer, J. L. Dehmer, J. B. West, and B. E. Cole, J. Phys. B **14**, 657 (1981).
- ¹⁹D. L. Ederer, A. C. Parr, B. E. Cole, R. Stockbauer, J. L. Dehmer, J. B. West, and K. Codling, Proc. R. Soc. London Ser. A **378**, 423 (1981).
- ²⁰J. B. West, K. Codling, A. C. Parr, D. L. Ederer, B. E. Cole, R. Stockbauer, and J. L. Dehmer, J. Phys. B **14**, 1791 (1981).
- ²¹A. C. Parr, D. M. P. Holland, D. L. Ederer, and J. L. Dehmer, Phys. Rev. A (submitted).
- ²²R. Unwin, I. Khan, N. Richardson, A. Bradshaw, K. Cederbaum, and W. Domke, Chem. Phys. Lett. **77**, 242 (1981).
- ²³M. I. Al-Joboury, D. P. May, and D. W. Turner, J. Chem. Soc. **1965**, 6350.
- ²⁴D. W. Turner and D. P. May, J. Chem. Phys. **46**, 1156 (1967).
- ²⁵J. H. D. Eland and C. J. Danby, Int. J. Mass Spectrom. Ion Phys. **1**, 111 (1968).
- ²⁶J. L. Bahr, A. J. Blake, J. H. Carver, J. L. Gardner, and V. Kumar, J. Quant. Spectros. Radiat. Transfer **12**, 59 (1972).
- ²⁷J. A. R. Samson, J. L. Gardner, and J. E. Mentall, J. Geophys. Res. **77**, 5560 (1972).
- ²⁸R. Frey, B. Gotchiev, O. F. Kulman, W. B. Peatman, H. Pollak, and E. W. Schlag, Chem. Phys. **21**, 89 (1973).
- ²⁹A. C. Parr, R. Stockbauer, B. E. Cole, D. L. Ederer, J. L. Dehmer, and J. B. West, Nucl. Instrum. Methods **172**, 357 (1980).
- ³⁰D. L. Ederer, B. E. Cole, and J. B. West, Nucl. Instrum. Methods **172**, 185 (1980).
- ³¹D. M. P. Holland, A. C. Parr, D. L. Ederer, J. L. Dehmer, and J. B. West, Nucl. Instrum. Methods (to be published).
- ³²D. W. Turner, C. Baker, A. D. Baker, and C. R. Brundle, *Handbook of Molecular Photoelectron Spectroscopy* (Wiley, New York, 1970).
- ³³T. E. Sharp and H. M. Rosenstock, J. Chem. Phys. **41**, 3453 (1964).
- ³⁴R. S. Berry and S. E. Neilson, Phys. Rev. A **1**, 383 (1970).
- ³⁵L. C. Lee and D. L. Judge, J. Chem. Phys. **57**, 4443 (1972).
- ³⁶T. Baer, Chemistry Department, University of North Carolina, Chapel Hill, NC 27514 and P. Guyon Lab, Collision Atomic et Moléculaire, Bat 351, University Paris-Sud, 91405 Orsay, France (unpublished, private communication).
- ³⁷See, for example, J. L. Dehmer and D. Dill, in *Electron-Molecule and Photon-Molecule Collisions*, edited by T. Rescigno, V. McKoy, and B. Schneider (Plenum, New York, 1979).
- ³⁸D. Dill and Ch. Jungen, J. Phys. Chem. **84**, 2116 (1980).
- ³⁹M. Raoult and Ch. Jungen, J. Chem. Phys. **74**, 3388 (1981).
- ⁴⁰P. M. Dehmer and W. A. Chupka, J. Chem. Phys. **65**, 2243 (1976).
- ⁴¹G. Raseeu, H. LeRouzo, and H. Lefebvre-Brion, J. Chem. Phys. **72**, 5701 (1980).
- ⁴²G. Raseeu, H. Lefebvre-Brion, H. Le Rouzo, and A. Roche, J. Chem. Phys. **74**, 6686 (1981).